Title

Eddy Covariance Evaluation of Ecosystem Fluxes at a Temperate Saltmarsh in Victoria, Australia Shows Large CO_2 Uptake

Authors

Ruth Reef[1],
Edoardo Daly[2,3],
Tivanka Anandappa[1],
Eboni-Jane Vienna-Hallam[1],
Harriet Robertson[1],
Matthew Peck[1],
Adrien Guyot[4,5]

Affiliations

1 School of Earth, Atmosphere and Environment, Monash University, VIC 3800, Australia
2 Department of Civil Engineering, Monash University, VIC 3800, Australia
3 WMAwater, Brisbane, QLD 4000, Australia
4 Atmospheric Observations Research Group, The University of Queensland, Brisbane, Australia
5 Australian Bureau of Meteorology, Melbourne, Australia

Corresponding Author

Associate Professor Ruth Reef
School of Earth Atmosphere and Environment
Monash University
9 Rainforest Walk, Clayton VIC 3800
Australia
Email: ruth.reef@monash.edu
Ph: +61 3 9905 8309

Key Points

This is the first study using eddy covariance to measure CO_2 fluxes at an Australian temperate saltmarsh, revealing temperature and light limitations to CO_2 uptake.

CO_2 fluxes varied seasonally; growing season net ecosystem productivity was 10.54 g CO_2 m^{-2} day^{-1}, dropping to 1.64 g CO_2 m^{-2} day^{-1} in winter.

Productivity at the French Island saltmarsh is high relative to global saltmarsh estimates but below global mangrove averages.

Deleted: Annual

Deleted: p

Deleted: estimated at 753 g C m^{-2} y^{-1}, surpassing

Abstract

Recent studies highlight the important role of vegetated coastal ecosystems in atmospheric carbon sequestration. Saltmarshes constitute 30% of these ecosystems globally and are the primary intertidal coastal wetland habitat outside the tropics. Eddy covariance (EC) is the main method for measuring biosphere-atmosphere fluxes, but its use in coastal environments is rare. At an Australian temperate saltmarsh site on French Island, Victoria, we measured CO_2 and water gas concentration gradients, temperature, wind speed and radiation. The marsh was dominated by a dense cover of *Sarcocornia quinqueflora*. Fluxes were seasonal, with minima in winter when vegetation is dormant. Net ecosystem productivity (NEP) during the growing season averaged 10.54 g CO_2 m^{-2} day^{-1} decreasing to 1.64 g CO_2 m^{-2} day^{-1} in the dormant period, yet the marsh remained a CO_2 sink due to some sempervirent species. Ecosystem respiration rates were lower during the dormant period compared with the growing season (1.00 vs 1.77 µmol CO_2 m^{-2} s^{-1}) with a slight positive relationship with temperature. During the growing season, fluxes were significantly influenced by light levels, ambient temperatures and humidity with cool temperatures and cloud cover limiting NEP. Ecosystem water use efficiency of 0.86 g C kg^{-1} H_2O was similar to other C3 intertidal marshes and evapotranspiration averaged 2.48 mm day^{-1} during the growing season.

Deleted: vegetation

Deleted: During the growing season, fluxes were significantly influenced by light levels, ambient temperatures and humidity. Evapotranspiration peaked at 0.27 mm h^{-1}. We cautiously estimate the annual NEP budget at this marsh to be 753 (±112.7) g C m^{-2} y^{-1} which is similar to carbon uptake by temperate saltmarshes in Europe and within the range measured at some US saltmarshes. This value is higher than the value hypothesised for global saltmarshes of 382 g C m^{-2} y^{-1} but is only half the mean value estimated for global mangroves.¶

EGUsphere Topics

Deleted: ¶

Emissions, Marine and Freshwater Biogeosciences, Earth System Biogeosciences

Short Summary

Studies show that saltmarshes excel at capturing carbon from the atmosphere. In this study, we measured CO_2 flux in an Australian temperate saltmarsh on French Island. The temperate saltmarsh exhibited strong seasonality. During the warmer growing season, the saltmarsh absorbed on average 10.5 grams of CO_2 from the atmosphere per m^2 daily. Even in winter, when plants were dormant, it continued to be a CO_2 sink, albeit smaller. Cool temperatures and high cloud cover inhibit carbon sequestration.

1. Introduction

Despite their relatively small global footprint of 54,650 km² (Mcowen et al., 2017), salt marshes provide a range of ecosystem services, including shoreline protection (Shepard et al., 2011), nutrient uptake, nursery grounds for fish populations (Whitfield, 2017) as well as functioning as significant carbon sinks through CO_2 uptake and storage in their organic rich sediments (McLeod et al., 2011). These 'blue carbon' habitats are recognised for their significant contribution to the global carbon cycle, as coastal wetlands more broadly are estimated to have accumulated more than a quarter of global organic soil carbon (Duarte, 2017).

Saltmarshes are a widely distributed intertidal habitat but are floristically divergent globally (Adam, 2002), such that commonalities in function and form do not extend across biogeographic realms. US saltmarshes, for example, are extensively dominated by a single grassy species, *Spartina alterniflora*, as opposed to the dominance of C_3 Chenopodioideae species in the southern hemisphere (Adam, 2002). Temperate saltmarshes occupy a latitudinal range spanning from approximately 30° to 60° (Mcowen et al., 2017) and are most commonly found along protected coastlines such as bays, estuaries, and lagoons, where they are sheltered from the full force of wave action (Mitsch and Gosselink, 2000). In the Southern Hemisphere, temperate saltmarshes have a strong Gondwanan element with high floristic similarity among the marshes of New Zealand, the southernmost coasts of South America and South Africa and the southern coastlines of Australia (Adam, 1990). These marshes are often associated with extensive seagrass meadows and mudflats, and in parts of their range, mangroves, forming complex coastal mosaics (Huxham et al., 2018). Saltmarshes have been heavily degraded across their range, and it is estimated that perhaps up to 50% of the global saltmarsh area has been lost since 1900 (Gedan et al., 2009), primarily due to land use change.

In most areas where they occur, seasonality plays a major role in the functioning of temperate saltmarshes (Ghosh and Mishra, 2017). These ecosystems experience distinct growing and dormant seasons, primarily driven by temperature, light availability, and precipitation patterns (Adam, 2000). During the growing season (typically spring and summer), increased temperatures and longer daylight hours stimulate plant growth, photosynthetic activity, and

Deleted: Seasonality

decomposition processes. Photosynthesis typically outpaces decomposition during this period, resulting in the temperate saltmarsh acting as a net CO_2 sink (Chmura et al., 2003). Conversely, the dormant season (usually fall and winter) is characterized by cooler temperatures and shorter days (Adam, 2000; Howe et al., 2010). These factors lead to reduced plant growth and photosynthetic activity (Adam, 2000) and while decomposition processes also slow down due to cooler temperatures, CO_2 release through decomposition often exceeds CO_2 uptake during this period (Artigas et al., 2015). In Australia, saltmarshes have been assumed to not exhibit seasonality (Owers et al., 2018) despite there being a scarcity of data on saltmarsh phenology and the implication this untested assumption could have on carbon budget estimations.

Gross primary production (GPP) of saltmarshes is the total amount of CO_2 uptake by plants through photosynthesis. Respiration (R_e) leads to a CO_2 flux directed back to the atmosphere due to all respiration processes occurring within the saltmarsh, involving both autotrophs and heterotrophs. The difference between these two fluxes is the net ecosystem exchange (NEE). Saltmarsh ecosystems can act as both sources and sinks of carbon dioxide (CO_2), influencing atmospheric CO_2 concentrations (Chmura et al., 2003). However, quantifying their net exchange remains challenging (Lu et al., 2017) hindering their effective inclusion in Earth System Models (Ward et al., 2020) and confounding the incorporation of saltmarsh restoration in emission reduction targets. Eddy covariance (EC) provides a powerful method for near-continuous, high-frequency monitoring of gas exchange between a vegetated surface and the atmosphere (Baldocchi, 2003), enabling the determination of net ecosystem exchange (NEE) of CO_2, and identifying the forcings that determine how CO_2 fluxes will respond to global climate change (Borges et al., 2006; Cai, 2011).

Previous EC studies in coastal saltmarshes have been focused on the Northern Hemisphere, in sites in the USA (e.g. Hill and Vargas, 2022; Kathilankal et al., 2008; Moffett et al., 2010; Nahrawi et al., 2020; Schäfer et al., 2019), France (Mayen et al., 2024), Japan (Otani and Endo, 2019) and China (Wei et al., 2020) but interest in the southern hemisphere is growing (Bautista et al., 2023). The NEE values from these studies indicate that there is high inter-site (as well as interannual, Erickson et al., (2013)) variability in carbon dynamics of saltmarshes, with a link to species types, salinity, hydrology (Moffett et al., 2010; Nahrawi et al., 2020), site specific biochemical conditions (Seyfferth et al., 2020) and latitude (Feagin et al., 2020). While generally considered important carbon sinks (e.g. ranging between 130 to 775 g C m^{-2}

Deleted: photosynthetic flux

Deleted: CO_2 from the atmosphere to the land surface, while respiration

Deleted: are limited to

Deleted:).

yr^{-1} in the USA, according to Kathilankal et al. (2008) and Wang et al,(2016) respectively) and globally hypothesised to average 382 g C m^{-2} y^{-1} (Alongi, 2020), some EC studies revealed saltmarshes to be net sources of CO_2 to the atmosphere (Vázquez-Lule and Vargas, 2021) especially in temperate saltmarshes that experience long dormant periods.

The aim of this study is to estimate CO_2 and water fluxes in a temperate saltmarsh in Victoria, southern Australia, to better characterise the effect of seasonality and environmental variables on the saltmarsh CO_2 budgets. This is the first study in an Australian coastal saltmarsh where CO_2 fluxes are estimated using the EC method.

2. Methods

2.82 Site Description

Deleted: 2.1

Formatted: List Paragraph, Outline numbered + Level: 2 + Numbering Style: 1, 2, 3, … + Start at: 82 + Alignment: Left + Aligned at: 0.63 cm + Indent at: 1.27 cm

Ecosystem flux measurements were collected at the Tortoise Head Ramsar coastal wetland on French Island, Victoria (38.388°S, 145.278°E, Fig. 1) within the Western Port embayment. French Island is within the Cfb climate zone (temperate oceanic climate) and experiences distinct seasonal variations in temperature and precipitation. Long term (30 year) climate data averaged from the nearby Cerberus Station (Australian Bureau of Meteorology, site 86361) indicated that summers, spanning from December through February, are generally mild to warm, with maximum temperatures typically ranging from 17°C to 25°C although occasional heatwaves lead to temporary spikes in temperature that can exceed 30°C. Winters, from June to September, are cooler, with maximum temperatures ranging between 7°C and 14°C and a mean minimum temperature of 6°C. Frost is infrequent due to maritime influence, though crisp mornings below 0°C occur 10% of the time in winter. Rainfall, evenly distributed throughout the year, averages ca. 715 mm y^{-1}, although in 2020 the site [1]ed higher than average rainfall (860 mm y^{-1}). The island is exposed to weather patterns influenced by the Southern Ocean and Bass Strait, leading to occasional storm systems, particularly in winter, bringing gusty winds and increased precipitation. Western Port has semi-diurnal tides with a range of nearly 3 m, resulting in wide intertidal flats occupied by mangroves of the species *Avicennia marina* and saltmarshes.

[1] Deleted: experienc

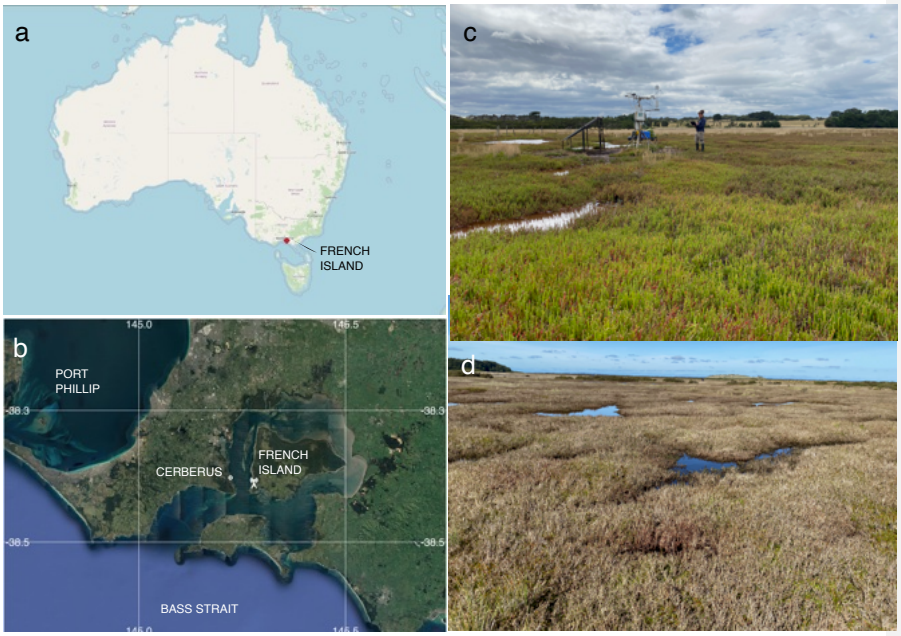

Figure 1: a) The location of French Island along the Bass Strait coast of Australia, and b) The location of the flux tower on French Island as well as the nearby Cerberus meteorological station (Bureau of Meteorology, Australia), © Google Earth. c) An image of the saltmarsh within the flux tower footprint during the growing season (with the tower and the author in the background), taken in February 2020 by Prudence Perry. d) an image of the saltmarsh during the dormant period, taken at the same location in September 2020 by Ruth Reef.

The site at French Island is dominated by an extensive temperate coastal saltmarsh community that is a particularly good natural representation of a broader biogeographic saltmarsh grouping which covers an area of ca. 7000 ha along Victoria's central coast embayments (Navarro et al., 2021). While the wetland at the site is a saltmarsh-mangrove-seagrass wetland system, the footprint of the flux tower was limited to the saltmarsh alone, which extends more than a kilometre from the shoreline in places. This geography provided the critical horizontally homogenous area with flat terrain required for ecosystem flux measurements. Floristically this saltmarsh is species poor, dominated by *Sarcocornia quinqeflora*. Stands of *Tecticornia arbuscula* are common in this saltmarsh, while *Atriplex cinerea*7pprox.7a*australia* and *Distichis distichophylla* can be prevalent depending on

Deleted: , *Suaeda*

elevation and soil drainage conditions. *Sarcocornia quinqeflora* is a perennial succulent and at the temperate ranges of its distribution it has a distinct growing season from October to May (Fig. 1c) when the stems turn red, followed by a woody and fibrous dormant period during the colder months of June through September (Fig. 1d). The height of the dominant vegetation ranged between 0.3 m.

2.83 2.2 Data Collection and Analysis

Eddy covariance measurements were made between November 2019 and August 2021 capturing both the saltmarsh growing season (October-May) as well as a dormant period (June-September). An array of standard micro-meteorological instruments included a 3-dimensional sonic anemometer (CSAT3, Campbell Scientific, USA), an open-path infra-red carbon dioxide (CO_2) gas and water vapour (H_2O) analyser (Li-7500, Li-Cor, USA) and 2 data-loggers. The tower was powered by a solar array with two accompanying 12V DC storage batteries. The sonic anemometer was mounted 2.3 m above ground. The CO_2/H2O gas analyser was mounted 0.11 m longitudinally displaced from the anemometer. A CR3000 datalogger (Campbell Scientific, USA), recorded the Li-7500, anemometer, short- and long-wave radiation (CNR4, Klip & Zonen, the Netherlands), air temperature and humidity (083E, Met One, USA) readings at 10 Hz frequency. Due to the location of the site in the Bass Strait (a region that experiences regular winter storms, high wind speeds and higher than national average cloud cover) the tower sustained damage due to winter storms several times during the deployment, as well as suffered periods of poor power supply due to short day lengths and high cloud cover; this was exacerbated by poor accessibility to the remote location during COVID-19 travel restrictions. The analysis thus focused on extended periods of continuous daily records and periods with large gaps in the dataset were removed.

Ecosystem fluxes were calculated for 30 min intervals using Eddy Pro software v.7 (LI-COR Inc., USA) Express Mode protocols. This processing step includes coordinate axis rotation correction, trend correction, data synchronisation, statistical tests for quality, density corrections and spectrum corrections. As part of this step, flux quality flags were assigned to the calculated CO_2 fluxes using the 0–2 flag policy 'Mauder and Foken 2004', based on the steady state test and the developed turbulent conditions test. The steady state test checks if fluxes remain consistent over the 30-minute averaging period by comparing the mean and

Deleted: -0.6

Formatted: List Paragraph, Outline numbered + Level: 2 + Numbering Style: 1, 2, 3, … + Start at: 82 + Alignment: Left + Aligned at: 0.63 cm + Indent at: 1.27 cm

Deleted: March

Deleted: April

Deleted: ,

standard deviation (SD) of fluxes in the first and second halves of the period. The developed turbulent conditions test ensures turbulence is well-developed and its energy spectra fits the Kolmogorov spectrum. Both tests assign partial flags that are combined into a single flag (0–2) in Eddy Pro, indicating the overall data quality. Only data that met the criteria of being in quality class 0 ('best quality fluxes') for CO_2 flux were chosen for further analysis. We further removed anomalous data points defined as values that exceed four SDs from the mean CO_2 flux; this resulted in the additional loss of ca. 1% of the dataset. Gap filling was not applied. Additional filtering was applied to nighttime data due to known weak convection at night, thus CO_2 flux data during periods of atmospheric stability, i.e. when night friction wind velocities (u*) were below 0.2 m s^{-1}, were excluded following inspection of the nightly NEE vs. u* curve to detect the threshold where NEE fall-off occurs. 0.2 m s^{-1} is the typical threshold value used in eddy-covariance studies (Davis et al., 2003). This resulted in a dataset of 674 day-time and 606 nighttime flux measurements during the dormant period and 4124 day-time and 3020 nighttime flux measurements for the growing period (Table 1). The growing season dataset included 90 days with 85% or more flux data coverage, while the dormant season dataset included 18 days, and these days were used for 24-hour flux integrations.

Deleted: standard deviations

Deleted: night-time

Deleted: .¶

Deleted: night-time

Deleted: night-time

Deleted: .

Table 1: Mean (±SD) net ecosystem exchange (µmol CO_2 m^{-2} s^{-1}) during day- and nighttime respectively, as well as the corresponding number of half hourly measurements from each month, following filter applications (n). Pink shading indicates the dormant season at the French Island saltmarsh.

Month	Daytime Mean NEE (SD); n	Nighttime Mean NEE (SD); n
October 2019	-2.29 (3.08); 121	2.04 (1.28); 70
November 2019	-1.84 (3.89); 151	2.85 (1.75); 110
December 2019	-3.33 (4.59); 96	1.14 (1.70); 15
January 2020	-1.31 (3.31); 63	2.10 (0.79); 27
February 2020	-3.83 (4.11); 540	1.89 (1.10); 280
March 2020	-3.86 (3.90); 494	1.63 (0.78); 351
August 2020	0.05 (2.05); 150	1.76 (1.22); 39
September 2020	-0.98 (2.04); 147	1.27 (0.96); 101
January 2021	-4.81 (5.04); 602	2.15 (1.55); 373
February 2021	-3.62 (4.27); 615	2.00 (1.19); 423
March 2021	-3.07 (3.95); 660	1.76 (1.20); 556
April 2021	-2.08 (3.02); 409	1.15 (0.87); 403

May 2021	-0.98 (2.57); 377	1.14 (1.04); 423
June 2021	0.58 (1.67); 271	0.93 (1.30); 328
July 2021	1.07 (1.38); 102	0.82 (0.62); 127

Half-hourly average CO_2 flux was measured in µmol m^{-2} s^{-1}, with positive fluxes indicating a flux direction from the Earth's surface to the atmosphere. Net ecosystem exchange (NEE) was defined as the net flux of CO_2 from the atmosphere to the marsh and was often negative during daytime, indicating that Gross Primary Productivity (GPP) was larger than ecosystem respiration (R_e). Evapotranspiration (ET) was calculated by Eddy Pro as the ratio between the latent heat flux (LE) and latent heat of vaporisation (λ). Ecosystem water use efficiency (WUEe) was then expressed as the ratio between daytime net ecosystem productivity in g CO_2 m^{-2} h^{-1} and evapotranspiration in mm h^{-1}.

A two-dimensional footprint estimation was provided according to the simple footprint parameterisation described in Kljun et al. (2015) calculating the ground position of the cumulative fraction of flux source contribution by distance for each 30-minute interval. We assessed the short-term effects of environmental factors on CO_2 fluxes at a half-hourly time scale (e.g. the effects of light, air temperature and vapour pressure deficit) using a series of non-linear or linear models. These analyses were limited to the growing season, when the plants were actively photosynthesising. To calculate the daily-integrated CO_2 and H_2O fluxes, the daily sum of these fluxes was determined for days with at least 85% data coverage. This involved using the trapezoid rule to estimate the area under the curve for each of these 24-hour periods. The trapezoid rule approximates the total flux by dividing the day into smaller intervals, each lasting 1,800 seconds. For each interval, the area is calculated by averaging the flux values at the beginning and end of the interval, then multiplying by the interval duration. These areas are then summed to obtain the total daily flux. This method ensures that even with some missing data points, a reliable estimate of the daily flux can be obtained. All post-processing and statistical analyses were performed in R 4.3.2 (R Core Team, 2024) including the packages *ggplto2*, *clifro*, *MASS*, *dismo*, *amerifluxr*, *rmarkdown*, *geosphere*, *ggmap* and *gbm*.

Because of the large data gaps, it was not possible to model the partition of the NEE in GEP and Re using common partitioning methods (Lasslop et al., 2010). For simplicity, it was

Deleted: The

Deleted: over time (i.e.,

Deleted: CO_2 or H_2O flux) were calculated

Deleted: complete records (

Deleted: density>80%) as

Deleted: period according to the trapezoid rule.

assumed that NEE at night coincided with R_e. R_e was corrected for temperature effects on respiration using a linear slope of the relationship between nighttime NEE and temperature. For the CO_2 budget, Net Ecosystem Production (NEP), was defined as NEP=-NEE.

Deleted: the

Deleted: night-time

Deleted: , and Gross Ecosystem Production (GEP), defined as GEP=-GPP, were used

3. Results

The observations were divided into a growing season and a dormant season to reflect the seasonal phenology of the dominant vegetation type within the flux tower footprint, which has a relatively short growing season during the summer. During the growing season, mean temperature averaged 22.3°C. Several heatwaves occurred during this period, with temperatures exceeding 40°C on a few occasions in 2019. The dormant season was significantly colder and windier, with frequent southerly winds (Fig. 2a). Footprint models showed a slight variation in flux source between the two seasons, although in both cases the size of the footprint and the vegetation composition within the footprint was similar (Figs. 2b and 2c), but the shape was skewed to the north during winter due to the prevalent southerly winds in that season (Fig. 2a). 70% of the flux measurement source was from within 50 m of the tower, while the maximum length of the source location was 73 m.

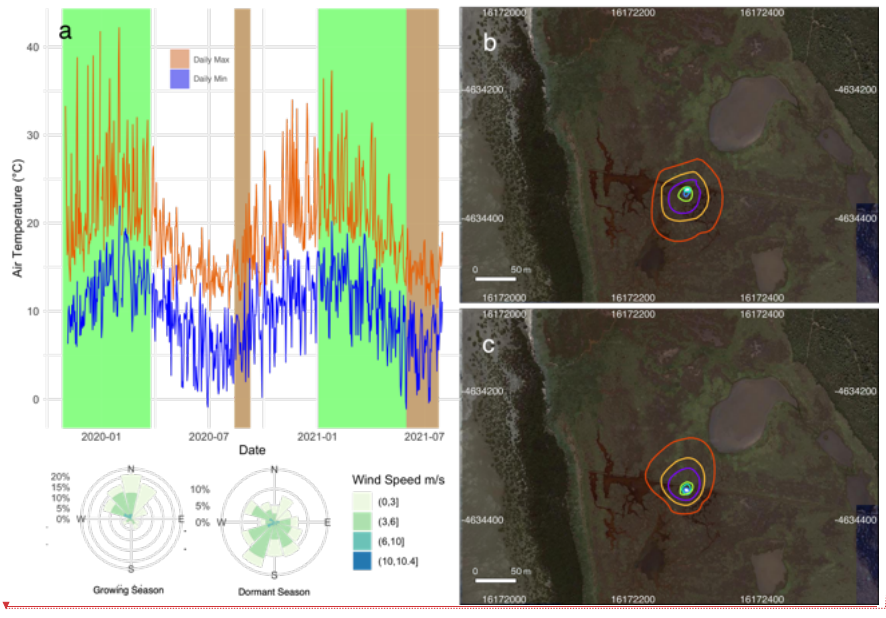

Deleted:

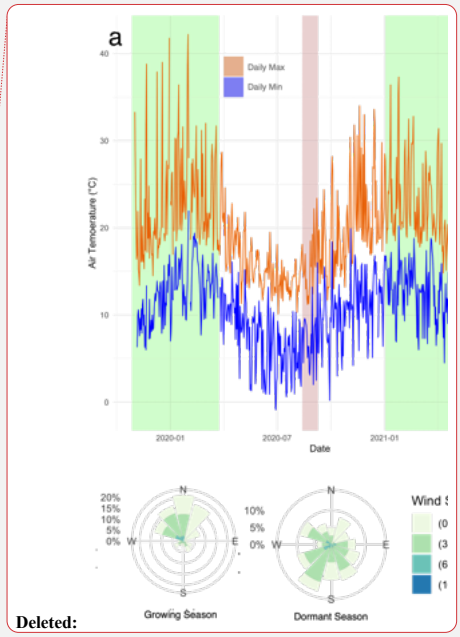

Figure 2: a) The minimum and maximum daily temperature recorded at the Cerberus meteorological station (Bureau of Meteorology, Fig. 1b) during 2019-2021. The marsh growing (October-May) and dormant (June-September) periods observed during this study are shaded in green and pink respectively. A corresponding wind rose diagram summarises the wind speeds and directions measured at the tower site during the observation periods. The flux source footprint surrounding the tower during the dormant season (b) and the growing season (c) shows the cumulative flux source contribution to the flux measurements, with the outer red line representing the distance by which 90% of the calculated flux is sourced and the other isolines from the tower outwards correspond to 10%, 20%, 40%, 60% and 80% of the flux.

The growing season dataset included 90 days with 85% or more flux data coverage, while the dormant season dataset included 18 days. There was a strong temporal variability in net ecosystem exchange (NEE) across both short (daily) and long (seasonal) temporal scales (Fig. 3). Daytime fluxes were defined as flux points where the global radiation values in the flux averaging half-hour interval were >12 W m^{-2} (as per EddyPro methodology). At the diurnal scale, saltmarsh NEE were negative mostly during the day and positive mostly during the night and ranged between -19.1 and 10.86 µmol m^{-2} s^{-1} across the measurement periods. Monthly averages and data coverage are shown in Table 1.

Deleted: Nov-Mar

Deleted: Aug-Sep

Deleted: highlighted

Deleted: 80

Deleted: .

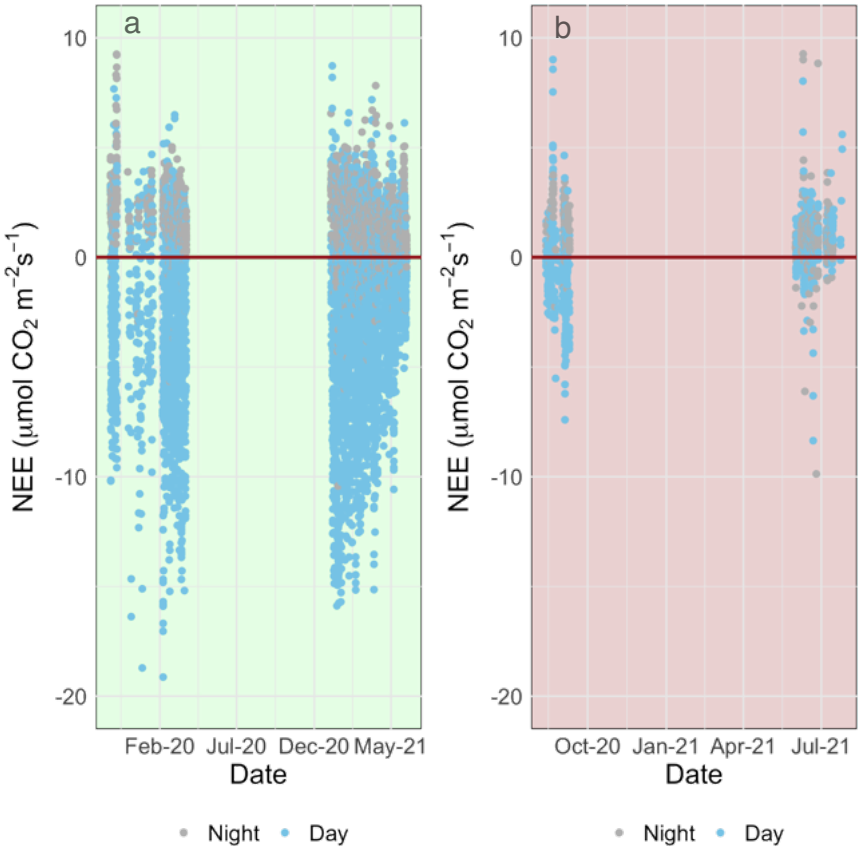

Figure 3: A time series of half-hourly measurements of CO_2 flux between a temperate saltmarsh and the atmosphere measured by eddy covariance during the marsh growing season (a) and the dormant season (b). Blue and grey points indicate measurements taken during daytime and nighttime respectively. Positive fluxes indicate a direction of flux from the Earth surface to the atmosphere.

Deleted: day-time

Deleted: night-time

Flux rates varied across the day, with CO_2 uptake peaking at 11:00 during the growing season, and later in the day (14:00) during the dormant period (Fig. 4). Ecosystem respiration rates (R_e, defined as nighttime CO_2 flux) were on average (±SD) 1.77 (±1.12) µmol m^{-2} s^{-1} during the growing season and 1.0 (± 0.93) µmol m^{-2} s^{-1} during the dormant period. The

Deleted: night-time

difference in ecosystem respiration between the growing and dormant seasons is highly significant (t-test, $p<0.01$). Daytime CO_2 flux was on average (±SD) -3.53 (± 4.15) µmol m^{-2} s^{-1} during the growing season and -0.25 (± 2.18) µmol m^{-2} s^{-1} during the dormant season. Thus, we derive that the maximum Gross Primary Productivity (GPP) of this ecosystem from NEE and temperature-corrected Re (Fig. 5), measured during the growing season, is ca. -5.34 ± 4.3 µmol CO_2 m^{-2} s^{-1} (-5.53 ± 4.45 g C m^{-2} day^{-1}). Average R_e is thus estimated to comprise 33% of GPP.

Deleted: ,

Mean (±SD) daily evapotranspiration was 2.48 mm (±2.79 mm) during the growing season and 0.97 mm (±1.35 mm) during the dormant season (Fig. 4). Evapotranspiration peaked at noon AEST during the growing season (0.26 mm h^{-1}), and later in the day (14:00 AEST) during the dormant season (0.14 mm h^{-1}).

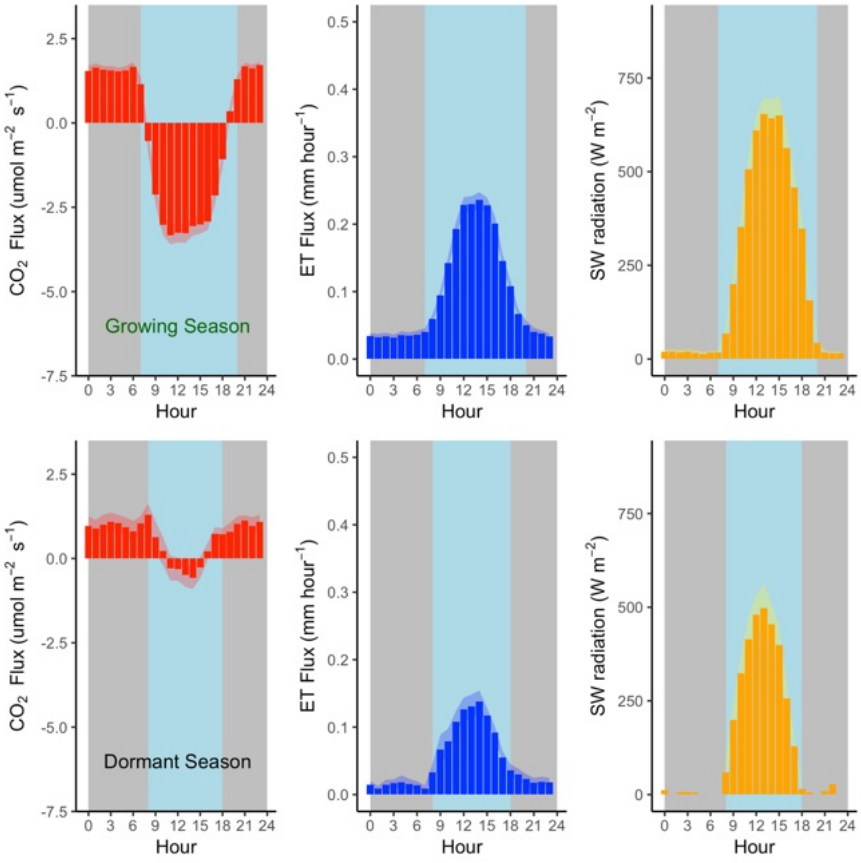

Figure 4: Mean hourly CO_2 and H_2O flux (evapotranspiration) rates during the growing season (top) and the dormant season (bottom) alongside mean short wave incoming radiation. Shading corresponds to 1 standard deviation (SD) around the mean. Grey plot background approximates nighttime periods, while light blue approximates daytime (actual day length varies within each season).

Deleted: night-time

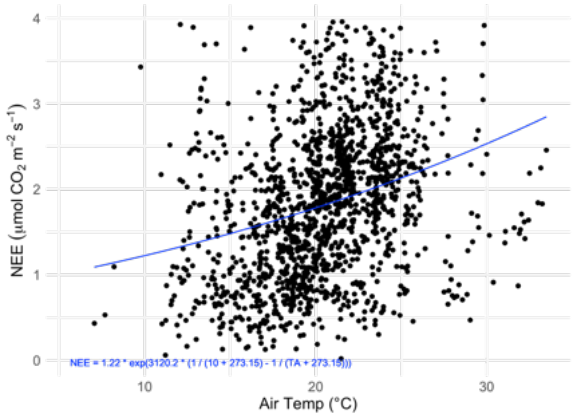

Figure 5: The relationship between nighttime half-hourly flux measurements (NEE) taken between the hours of 22:00 and 02:00 and air temperature (TA). The fitted curve (blue line) is the fitted Lloyd & Taylor Arrhenius non-linear model: NEE = 1.22*exp(3120.2*(1/283.2-1/(TA+273.2))), R^2 = 0.09.

The effect of some environmental forcings on daytime NEE during the saltmarsh growing season were explored (Fig. 6). To distinguish this daytime-only value from the 24-hour carbon balance integration, and to better highlight CO_2 uptake, NEP values are shown.

Short wave radiation (visible light) was a limiting factor to NEP below approximately 300 W m^{-2}, but radiation did not reach damaging levels that would lead to a drop in NEP throughout the measurement range, which reached a maximum level of ca. 800 W m^{-2}. Unlike light, the NEP-air temperature relationship followed a Gaussian response, with the highest NEP achieved at the optimal temperature of 25.3°C with a SD of 3.8°C followed by a decline in CO_2 uptake by the marsh at higher temperatures. The minimum and maximum air temperatures for which modelled NEP nears zero (defined here as 3 SDs from the mean) are 13.9°C and 36.7°C respectively. Temperature also had a slight but significant positive linear relationship with ecosystem respiration (slope=0.07 µmol CO_2 m^{-2} s^{-1} $°C^{-1}$, $p<0.01$, data not shown).

Deleted: 5

Deleted: standard deviation

Deleted: standard deviations

NEP was positively correlated with evapotranspiration during the growing season (Pearson r = 0.59, Fig. 6 C). The slope of the NEP/ET relationship was 20.0, indicating an ecosystem water use efficiency (WUE_e) of 0.86 g C kg^{-1} H_2O (R^2 = 0.34, p<0.001). The response of NEP to atmospheric vapour pressure deficit (VPD) fit a Gaussian relationship (the commonly observed inverse U-shaped curve relationship in response to VPD in plants), with NEP declining rapidly when VPD exceeded 2.39 kPa. The optimal range of VPD within which NEP was maximised in this ecosystem was 1.92 kPa (±0.73 kPa).

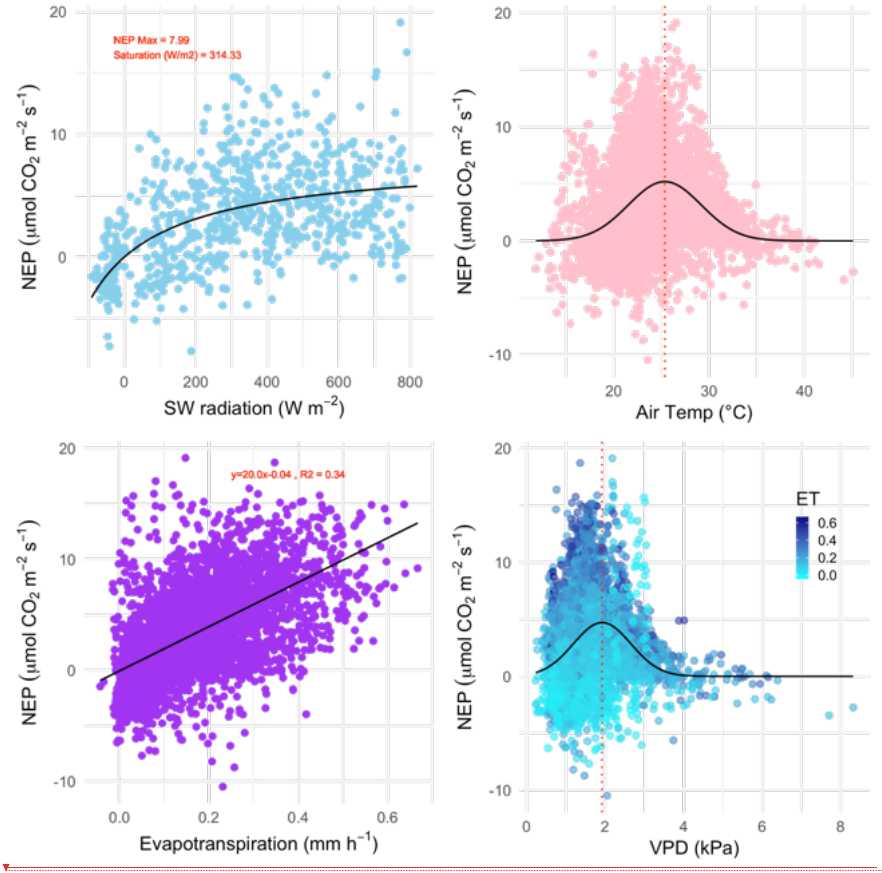

Figure 6: The relationship between growing season daytime half-hourly values of net ecosystem productivity (NEP, µmol CO_2 m^{-2} s^{-1}) and corresponding environmental variables. a) Net shortwave (SW) radiation (visible light); black line is the Michaelis-Menten model of

Deleted: 5

Deleted:

Deleted: 5

Deleted: CO_2 uptake

Deleted: Shortwave

best fit. The coefficient of saturation is at 314 W m^{-2} and maximum net productivity is 8.0 µmol CO_2 m^{-2} s^{-1}. b) Air temperature; black line is a Gaussian model of best fit with a temperature optimum at 25.3°C. c) Evapotranspiration; linear model (R^2 = 0.34) has a slope of 20.0. d) Vapour Pressure Deficit; black line is a Gaussian model of best fit with a VPD optimum at 1.92 kPa, points are coloured by the level of evapotranspiration during the half hourly NEP measurement.

When integrated over a 24-hour period, the saltmarsh is on average a daily CO_2 sink during all canopy phenological phases (Fig. 7), although during the dormant season the sink is weaker, with an average uptake of -2.42 g CO_2 m^{-2} day^{-1} (±2.54). During the growing season (defined as the non-dormant period and thus reflecting several phenological stages), the marsh is a substantial sink with a mean (±SD) daily NEP of 10.95 g CO_2 m^{-2} day^{-1} (±4.98) over a 24-hour period (ranging between -22.8 and 4.3 g of CO_2 emission to the atmosphere m^{-2} day^{-1}) . The daily CO_2 budget during the growing season showed some variability among days (CV=0.46, Fig. 7) and days with lower average light levels (i.e. cloudy days) had a significant negative impact on the CO_2 budget (multiple linear regression, $p < 0.02$, R^2 = 0.27). Daily maximum air temperatures did not have a significant impact on the daily CO_2 budget ($p = 0.77$) at this location, although NEE was significantly affected by temperature at finer temporal scales (Figure 6).

Deleted: .

Deleted: 6

Deleted: 6

Deleted: 5). Assuming the dormant period spans a third of the year, we cautiously estimate an annual NEP value of 753 (±112.7) g C m^{-2} yr^{-1} .

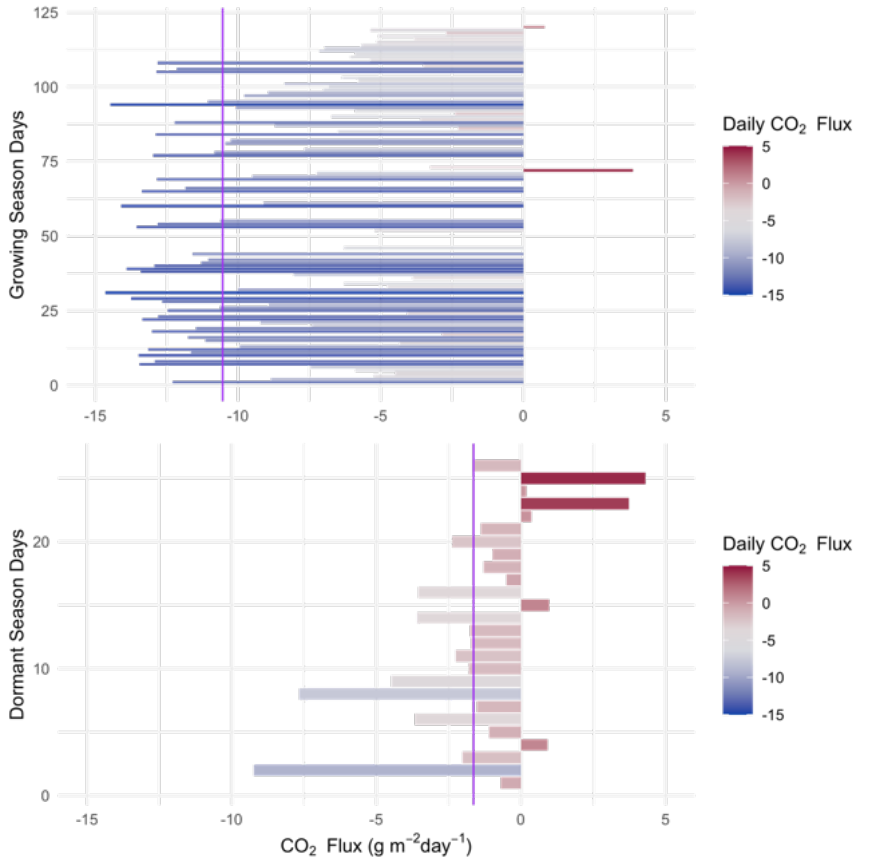

Figure 7: Daily (24 h) integrated NEE in g CO_2 m^{-2} day^{-1} during the saltmarsh growing season (top) and the dormant season (bottom) for days with data density > 85%. Purple lines indicate the mean daily integrated flux for each season (-10.54 and -1.64 g CO_2 m^{-2} day^{-1} with an SD of 4.98 and 2.54 for growing and dormant respectively). A positive balance indicates an integrated net flux of CO_2 from the Earth's surface to the atmosphere over the 24-hour period.

4. Discussion

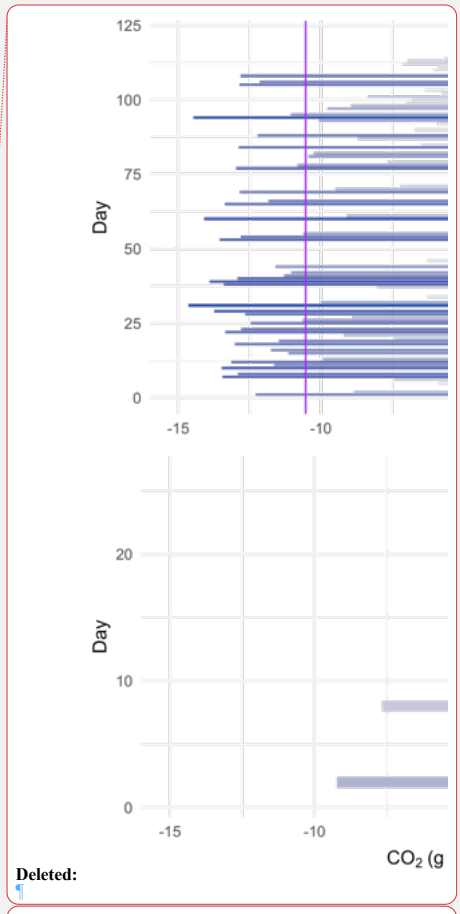

Deleted:

Deleted: 6

Deleted: Assuming the dormant season period spans one third of the year, we cautiously estimate an annual NEP value of 753 g C m^{-2} yr^{-1} (±weighted sum of SD of 5.9).

The study provided high-frequency measurements of an abundant greenhouse gas (CO_2) using a precise technique (eddy covariance flux) in an ecosystem with limited historical measurements. Time series analysis was performed on CO_2 flux measurements across various scales (daily, nightly, diel, half-hourly, hourly, seasonally) to assess the impacts of ET, SW Rad, VPD, and Tair on CO_2 flux and how these relationships change throughout the year. Seasonality was observed for the first time in an Australian saltmarsh and had a significant effect on carbon and water flux. Growing season net ecosystem productivity was five times greater than during the dormant period. Seasonality in Australian marshes has not been previously reported in the scientific literature and contradicts previous assumptions that Australian saltmarshes do not exhibit the growing and dormant phenology observed on other continents (Clarke and Jacoby, 1994). Seasonality had a significant impact on the carbon budget in this marsh and is an important characteristic of this habitat that has been overlooked (Owers et al., 2018). Seasonality can also have other broader implications yet to be considered in Australian marshes. For example, in the USA, the saltmarsh greening up period was shown to be an important range-wide timing event for migratory birds (Smith et al., 2020) with plant-growth metrics predicting the timing of nest initiation for shorebirds. Saltmarshes in Australia are important roosting and feeding sites along the East Asian Australasian Flyway, particularly for waders, thus potentially a similar relationship between migration timing and saltmarsh phenology could be occurring. Seasonality also affects other significant ecosystem functions such as the bio-geomorphological feedback between saltmarshes, coastal hydrodynamics and landscape evolution (Reents et al., 2022).

We derived the light-response and associated coefficients of light regulation of saltmarsh NEE using the Michaelis Menten model (Chen et al., 2002). Quantum (or production) efficiency is the predominant input in remote sensing techniques to model productivity, and is specific to the biome (Hilker et al., 2010). While not directly comparable to leaf level quantum efficiency measurements, the quantum efficiency (α) of the NEP light response curve was estimated from the slope of the Michaelis-Menten model to be 0.025 µmol CO_2 J^{-1}. The ecosystem reached light saturation at an insolation of 314 W m^{-2}, but daytime insolation was below this value more than 50% of the time suggesting that light might be a significant limiting factor to NEP at this marsh, especially during winter. The level of light limitation we observed is an underestimation, due to the loss of high-quality EC data during periods of rain. The solar geometry at this latitude and the length of day result in an annual average top of

Deleted: At this temperate saltmarsh, seasonality

Deleted: ,

Deleted: were made

Deleted: ¶

Deleted: might be an overlooked

Deleted: and in addition to affecting flux estimations,

atmosphere SW radiation of 250 W m^{-2}, but clouds can strongly modulate the SW radiation balance (SWCRE), and apart from the months of January and February when cloudy days are less frequent (10-12 days per month), cloudy days are frequent at this site, averaging 15-17 days per month (Bureau of Meteorology) and could significantly impact on NEP.

Temperature is another forcing that significantly impacts NEE at this marsh, with an optimal range for maximum NEP at 25.3°C (21.5°C-29.1°C). Data for Australian saltmarshes is not available, but this optimal temperature response range is similar to that measured experimentally in a saltmarsh species in an equivalent climate zone (e.g. Georgia, (Giurgevich and Dunn, 1981)) and to the values hypothesised for the habitat from data collected along the US Atlantic Coast, (Feher et al., 2017). The long-term average maximum daytime temperature at this site is 19.2°C, which is cooler than the optimal range for NEE suggesting temperature can be a significant limiting factor to productivity, especially during the dormancy period where average monthly maximum temperatures are only 13.7°C to 16.6°C (Bureau of Meteorology). During the growing season the average maximum temperatures are within the range of optimal NEE (20.6°C to 23.1°C), although hot days (>30°C) significantly depress NEE and depending on the year, can be common during summer months (averaging 2-6 days per month). Within the diversity of saltmarsh species found globally, some species have C4 photosynthetic pathways (Drake, 1989). C4 photosynthesis plants often exhibit higher optimum temperature ranges (30-35°C, Berry and Björkman, 1980) than C3 photosynthesis plants (20-25), and the cooler conditions at this site could explain the absence of C4 plants from this bioregion. The parabolic relationship between NEP and air temperature and NEP and VPD suggest that higher air temperatures and VPD (which are expected with climate change) could negatively impact CO_2 uptake by these coastal ecosystems. High VPD was related to lower NEP, and to a lesser extent, lower ET (Fig. 6d). However, VPD increases atmospheric demand for water, increasing the evaporation from the saturated marsh surfaces in the footprint, and this atmospheric demand could be forcing ET at high VPD rather than plant moderation via reduced transpiration, even if transpiration is reduced. Thus, despite maintained ET during VPD periods we cannot conclude a non-closure of stomata. NEP also reduced below a VPD of 1.92 KPa, but at our field site low VPD correlated with low temperatures (r = 0.88), and low temperatures were shown to limit NEP.

Deleted: ¶

In saltmarshes, evapotranspiration occurs from plant mediated transpiration but also from soil pores (which tend to be saturated), wetted leaves and open water. We observed average evaporation rates of 2.48 mm day^{-1} during the growing season and 0.97 mm day^{-1} during the dormant season. Actual evapotranspiration in this region modelled using the CMRSET algorithm is estimated to range between 0.6 and 3.2 mm day^{-1} during winter and summer respectively (McVicar et al., 2022); our field measurements support the model. Overall, rainfall is in excess of the requirements for maintaining ET at this site, although deficits can develop for short periods during the growing season, when ET is higher, perhaps explaining the drier saltmarsh surface during this period. Conversely, long term rainfall excess could be contributing to the complicated hydrology at this location, where inundation is not strictly associated with tidal stage (data not shown) and our observation of long (5-day) periods of inundation during winter.

Growing season ET rates are significantly higher than those of the dormant season, partly due to the solar configuration in winter as opposed to summer, but also due to phenological changes. A big leaf model estimation of evapotranspiration from saltmarshes in New South Wales estimates ET to be highly sensitive to vegetation height, increasing by more than 1 mm day^{-1} as vegetation height increases from 0.1 to 0.4 m (Hughes et al., 2001) and transpiration in saltmarsh plants in the cold season has been shown to account for only 20% of the annual transpiration budget (Giurgevich and Dunn, 1981) following the same pattern as the seasonal distribution of productivity.

The rate of carbon uptake per unit of water loss (WUE) is a key ecosystem characteristic, which is a result of a suite of physical and canopy physiological forcings, and has direct implications for ecosystem function and global water and carbon cycling. Mean water use efficiency (WUEe) of this saltmarsh was estimated at 0.86 g C kg^{-1} H_2O, which is markedly lower than for grass dominated saltmarshes in China (2.9 g C kg^{-1} H_2O, Xiao et al. (2013)) but similar to the value for WUEe based on NEP and ET in mangroves (0.77 g C kg^{-1} H_2O, Krauss et al. (2022)), which are also C3 plants. The Chinese saltmarshes studied in Xiao et al. (2013) are dominated by *Spartina alterniflora*, a C4 perennial grass. C4 plants have higher (often double) water use efficiencies than C3 plants due to CO_2 concentrating mechanisms (Osborne and Freckleton, 2009). The saltmarsh at French Island includes only C3 plants, and the dominant chenopod *Sarcocornia quinqueflora* has been suspected to have higher evapotranspiration rates than saltmarsh by approx. 15% (Hughes et al., 2001), but while

Deleted: these values are consistent with

Deleted: . ¶
Long

Deleted:).

Deleted: (2022)). The

Deleted: grasses

Sarcocornia quinqueflora dominates at this site, the footprint is a mix of species, and the lower WUEe cannot be directly linked to the presence of *Sarcocornia quinqueflora*. Furthermore, like most wetlands, the wetland surface is a mixed composition of emergent vegetation, unsaturated soil and water bodies thus the spatial scale at which WUEe is determined encompasses both the canopy (Ec) as well as any open water present in the footprint. Transpiration is predicted to account for only 55% of ET in these systems (Hughes et al., 2001), which is an Ec to ET ratio similar to that of mangroves (Krauss et al., 2022) but significantly lower than terrestrial forests where more than 90% of ET can be attributed to transpiration. Thus, regional variations in WUEe can be attributed to multiple forcings that form complex spatiotemporal patterns.

Saltmarshes are considered among the most productive ecosystems on Earth with an estimated global NEP of 634 Tg C y^{-1} (Fagherazzi et al., 2013) and 601 634 Tg C y^{-1} (Rosentreter et al., 2023). Productivity of southern Australian marshes was previously estimated at 0.8 kg m^{-2} y^{-1} by repeated measurements of above ground standing crops (Clarke and Jacoby, 1994), which if not accounting for season, equates to 2.2 g C m^{-2} d^{-1}. Similar studies on saltmarshes in France report lower productivity (483 g C m^{-2} y^{-1}, (Mayen et al., 2024)) and daily growing season rates of 1.53 g C m^{-2} d^{-1}, but mid-latitude saltmarsh sites in the USA and China show productivity rates of 775 g C m^{-2} y^{-1}, (Wang et al., 2016) and 668 g C m^{-2} y^{-1}, (Xiao et al., 2013) respectively. It is clear that productivity across climate zones and biogeographic regions varies widely with some studies even reporting net emissions over an annual period from some marshes and a global average estimated between 382 (Alongi, 2020) and 1,585 g C m^{-2} y^{-1} (Chmura et al., 2003), albeit based on a small subset of studies. An analysis of GPP across latitudes in the USA show that warmer sites (including mangrove wetlands in southern USA) had significantly higher GPP than mid-latitude saltmarshes such as the one on French Island (Feagin et al., 2020). Mangroves have higher NEE than saltmarshes, estimated by Krauss et al. (2022) to average 1200 g C m^{-2} y^{-1}. While our data does not provide enough coverage for a long-term annual estimate of carbon flux, our daily values of an average of 2.88 g C m^{-2} d^{-1} during the growing season, combined with the relatively short dormant season relative to other temperate locations, suggest a high carbon sequestration rate for this ecosystem type. In another southern hemisphere study, growing season rates at an EC tower site in Argentina, are extrapolated by us to average 1.6 g C m^{-2} d^{-1} (Bautista et al., 2023) but in that saltmarsh, flooding reduced vegetation biomass and productivity.

Formatted: Not Superscript/ Subscript

Deleted: is remarkably similar

Deleted: the values reported here, where we extrapolate an approximate annual mean of 0.75 kg C m-

Deleted: y

Formatted: Not Superscript/ Subscript

Deleted: than the marshes at French Island (-

Deleted: but our values are within the range reported for

Deleted: (-

Deleted:))

Deleted: China (-

Deleted:)).

Deleted: -

Deleted: -

Deleted: (Krauss et al., 2022) to average 1200 g C m^{-2} y^{-1}.

The data presented here is the exchange of carbon between the land surface and the atmosphere, but saltmarshes, like other marine connected communities, exchange carbon also through dissolved carbon pathways, which can be significant (Cai, 2011). Thus, the fluxes presented here do not constitute the entire carbon budget of this ecosystem.

5. Conclusions

The response of the French Island saltmarsh to environmental drivers is indicative of the complex interactions determining saltmarsh productivity. The unique long-term, high-resolution record enabled us to derive temperature, VPD and light response functions, thus formulating equations that describe how climate-change sensitive parameters such as temperature, relative humidity, and cloud cover, affect CO_2 uptake, respiration and evapotranspiration. The marsh operated as a CO_2 sink throughout the various canopy phenological phases, but during the dormant period, CO_2 uptake was less than 25% that of the growing season. Seasonality of greenhouse gas fluxes in Australian saltmarshes is an understudied but important aspect of global carbon budgeting.

Deleted: While the overall carbon sequestration rate we measured was in the range of other temperate saltmarsh estimates (ca. 750 g C m^{-2} y^{-1}),

Deleted: t

Deleted: has not been previously considered

Deleted: and it should not be overlooked when estimating saltmarsh

Deleted: budgets

Competing interests

The contact author has declared that none of the authors has any competing interests.

Formatted: Font: Times New Roman, 12 pt

Acknowledgments

The work was carried out with the permission of Parks Victoria (Permit 10008684). We thank Phil and Yuko Bock for logistic support and accommodation on French Island. We thank Leigh Burgess, Kiri Mason and Ian McHugh for technical support and the Australian OzFlux community for ongoing collaboration. This work was funded by an Australian Research Council Discovery Award to RR and ED (DP220102873) as well as a Monash University Networks of Excellence award to RR.

Data Availability

Data used for this analysis is available at https://figshare.com/s/ba62aafd1a4049248a08 (note that this is a temporary private link to an embargoed dataset which will be replaced with a publicly available DOI upon publication).

Author contribution

RR conceptualised the study, acquired funding, prepared the manuscript, designed and carried out the field campaign, and performed the analysis. ED acquired funding, developed methodology and prepared the manuscript. AG developed methodology and prepared the manuscript. TA, EJVH, HR and MP were involved in the field investigation and administration of the project and provided edits on the manuscript.

References

Adam, P.: Saltmarsh Ecology, Cambridge University Press, 1990.

Adam, P.: Morecambe Bay saltmarshes: 25 years of change, in: British Saltmarshes, Forrest Text, Cardigan, UK, 81–107, 2000.

Adam, P.: Saltmarshes in a time of change, Environ. Conserv., 29, 39–61, https://doi.org/10.1017/S0376892902000048, 2002.

Alongi, D. M.: Carbon balance in salt marsh and mangrove ecosystems: A global synthesis, J. Mar. Sci. Eng., 8, 767, 2020.

Artigas, F., Shin, J. Y., Hobble, C., Marti-Donati, A., Schäfer, K. V. R., and Pechmann, I.: Long term carbon storage potential and CO_2 sink strength of a restored salt marsh in New Jersey, Agric. For. Meteorol., 200, 313–321, https://doi.org/10.1016/j.agrformet.2014.09.012, 2015.

Baldocchi, D. D.: Assessing the eddy covariance technique for evaluating carbon dioxide exchange rates of ecosystems: past, present and future, Glob. Change Biol., 9, 479–492, https://doi.org/10.1046/j.1365-2486.2003.00629.x, 2003.

Bautista, N. E., Gassmann, M. I. , and Pérez, C. F.: Gross primary production, ecosystem respiration, and net ecosystem production in a southeastern South American salt marsh. Estuaries Coast, 46, 1923-1937, https://doi.org/10.1007/s12237-023-01224-8, 2023.

Berry, J., and Björkman, O.: Photosynthetic response and adaptation to temperature in higher plants, Ann. Rev. Plant Physiol., 31, 491-543, https://doi.org/10.1146/annurev.pp.31.060180.002423, 1980.

Borges, A. V., Schiettecatte, L.-S., Abril, G., Delille, B., and Gazeau, F.: Carbon dioxide in European coastal waters, Trace Gases Eur. Coast. Zone, 70, 375–387, https://doi.org/10.1016/j.ecss.2006.05.046, 2006.

740 Cai, W.-J.: Estuarine and coastal ocean carbon paradox: CO_2 sinks or sites of terrestrial
741 carbon incineration?, Annu. Rev. Mar. Sci., 3, 123–145, https://doi.org/10.1146/annurev-
742 marine-120709-142723, 2011.

743 Chen, J., Falk, M., Euskirchen, E., Paw U, K. T., Suchanek, T. H., Ustin, S. L., Bond, B. J.,
744 Brosofske, K. D., Phillips, N., and Bi, R.: Biophysical controls of carbon flows in three
745 successional Douglas-fir stands based on eddy-covariance measurements, Tree Physiol., 22,
746 169–177, https://doi.org/10.1093/treephys/22.2-3.169, 2002.

747 Chmura, G. L., Anisfeld, S. C., Cahoon, D. R., and Lynch, J. C.: Global carbon sequestration
748 in tidal, saline wetland soils, Glob. Biogeochem. Cycles, 17,
749 https://doi.org/10.1029/2002GB001917, 2003.

750 Clarke, P., J. and Jacoby, C. A.: Biomass and above-ground productivity of salt-marsh plants
751 in South-eastern Australia, Aust. J. Mar. Freshw. Res., 45, 1521–1528, 1994.

752 Davis, K. J., Bakwin, P. S., Yi, C., Berger, B. W., Zhao, C., Teclaw, R. M., and Isebrands, J.
753 G.: The annual cycles of CO_2 and H_2O exchange over a northern mixed forest as observed
754 from a very tall tower, Glob. Change Biol., 9, 1241-1332, https://doi.org/10.1046/j.1365-
755 2486.2003.00672.x, 2003.

756 Drake, B. G.: Photosynthesis of salt marsh species, Aquat. Bot., 34, 167-180,
757 https://doi.org/10.1016/0304-3770(89)90055-7, 1989.
758
759 Duarte, C. M.: Reviews and syntheses: Hidden forests, the role of vegetated coastal habitats
760 in the ocean carbon budget, Biogeosciences, 14, 301–310, https://doi.org/10.5194/bg-14-301-
761 2017, 2017.

762 Erickson, J. E., Peresta, G., Montovan, K. J., and Drake, B. G.: Direct and indirect effects of
763 elevated atmospheric CO_2 on net ecosystem production in a Chesapeake Bay tidal wetland,
764 Glob. Change Biol., 19, 3368–3378, 2013.

765 Fagherazzi, S., Wiberg, P. L., Temmerman, S., Struyf, E., Zhao, Y., and Raymond, P. A.:
766 Fluxes of water, sediments, and biogeochemical compounds in salt marshes, Ecol. Process.,
767 2, 3, https://doi.org/10.1186/2192-1709-2-3, 2013.

768 Feagin, R. A., Forbrich, I., Huff, T. P., Barr, J. G., Ruiz-Plancarte, J., Fuentes, J. D., Najjar,
769 R. G., Vargas, R., Vázquez-Lule, A., Windham-Myers, L., Kroeger, K. D., Ward, E. J.,
770 Moore, G. W., Leclerc, M., Krauss, K. W., Stagg, C. L., Alber, M., Knox, S. H., Schäfer, K.
771 V. R., Bianchi, T. S., Hutchings, J. A., Nahrawi, H., Noormets, A., Mitra, B., Jaimes, A.,
772 Hinson, A. L., Bergamaschi, B., King, J. S., and Miao, G.: Tidal wetland gross primary
773 production across the continental United States, 2000–2019, Glob. Biogeochem. Cycles, 34,
774 e2019GB006349, https://doi.org/10.1029/2019GB006349, 2020.

775 Feher, L. C., Osland, M. J., Griffith, K. T., Grace, J. B., Howard, R. J., Stagg, C. L.,
776 Enwright, N. M., Krauss, K. W., Gabler, C. A., Day, R. H., and Rogers, K.: Linear and
777 nonlinear effects of temperature and precipitation on ecosystem properties in tidal saline
778 wetlands, Ecosphere, 8, e01956, https://doi.org/10.1002/ecs2.1956, 2017.

779 Gedan, K. B., Silliman, B. R., and Bertness, M. D.: Centuries of human-driven change in salt
780 marsh ecosystems, Annu. Rev. Mar. Sci., 1, 117–141,
781 https://doi.org/10.1146/annurev.marine.010908.163930, 2009.

782 Ghosh, S. and Mishra, D. R.: Analyzing the long-term phenological trends of salt marsh
783 ecosystem across coastal Louisiana, Remote Sens., 9, https://doi.org/10.3390/rs9121340,
784 2017.

785 Giurgevich, J. R. and Dunn, E. L.: A comparative analysis of the CO_2 and water vapor
786 responses of two Spartina species from Georgia coastal marshes, Estuar. Coast. Shelf Sci.,
787 12, 561–568, https://doi.org/10.1016/S0302-3524(81)80082-5, 1981.

788 Hilker, T., Hall, F. G., Coops, N. C., Lyapustin, A., Wang, Y., Nesic, Z., Grant, N., Black, T.
789 A., Wulder, M. A., Kljun, N., Hopkinson, C., and Chasmer, L.: Remote sensing of
790 photosynthetic light-use efficiency across two forested biomes: Spatial scaling, Remote Sens.
791 Environ., 114, 2863–2874, https://doi.org/10.1016/j.rse.2010.07.004, 2010.

792 Hill, A. C. and Vargas, R.: Methane and carbon dioxide fluxes in a temperate tidal salt marsh:
793 comparisons between plot and ecosystem measurements, J. Geophys. Res. Biogeosciences,
794 127, e2022JG006943, https://doi.org/10.1029/2022JG006943, 2022.

795 Howe, A. J., Rodríguez, J. F., Spencer, J., MacFarlane, G. R., and Saintilan, N.: Response of
796 estuarine wetlands to reinstatement of tidal flows, Mar. Freshw. Res., 61, 702–713, 2010.

797 Hughes, C. E., Kalma, J. D., Binning, P., Willgoose, G. R., and Vertzonis, M.: Estimating
798 evapotranspiration for a temperate salt marsh, Newcastle, Australia, Hydrol. Process., 15,
799 957–975, https://doi.org/10.1002/hyp.189, 2001.

800 Huxham, M., Whitlock, D., Githaiga, M., and Dencer-Brown, A.: Carbon in the coastal
801 seascape: how interactions between mangrove forests, seagrass meadows and tidal marshes
802 influence carbon storage, Curr. For. Rep., 4, 101–110, https://doi.org/10.1007/s40725-018-
803 0077-4, 2018.

804 Kathilankal, J. C., Mozdzer, T. J., Fuentes, J. D., D'Odorico, P., McGlathery, K. J., and
805 Zieman, J. C.: Tidal influences on carbon assimilation by a salt marsh, Environ. Res. Lett., 3,
806 044010, https://doi.org/10.1088/1748-9326/3/4/044010, 2008.

807 Kljun, N., Calanca, P., Rotach, M. W., and Schmid, H. P.: A simple two-dimensional
808 parameterisation for Flux Footprint Prediction (FFP), Geosci Model Dev, 8, 3695–3713,
809 https://doi.org/10.5194/gmd-8-3695-2015, 2015.

810 Krauss, K. W., Lovelock, C. E., Chen, L., Berger, U., Ball, M. C., Reef, R., Peters, R.,
811 Bowen, H., Vovides, A. G., Ward, E. J., and others: Mangroves provide blue carbon
812 ecological value at a low freshwater cost, Sci. Rep., 12, https-doi, 2022.

813 Lasslop, G., Reichstein, M., Papale, D., Richardson, A. D., Arneth, A., BARR, A., STOY, P.,
814 and WOHLFAHRT, G.: Separation of net ecosystem exchange into assimilation and
815 respiration using a light response curve approach: critical issues and global evaluation, Glob.
816 Change Biol., 16, 187–208, https://doi.org/10.1111/j.1365-2486.2009.02041.x, 2010.

817 Lu, W., Xiao, J., Liu, F., Zhang, Y., Liu, C., and Lin, G.: Contrasting ecosystem CO_2 fluxes
818 of inland and coastal wetlands: a meta-analysis of eddy covariance data, Glob. Change Biol.,
819 23, 1180–1198, https://doi.org/10.1111/gcb.13424, 2017.

820 Massamann, A., Gentine, P., and Lin, C.: When does vapour pressure deficit drive or reduce
821 evapotranspiration? J. Adv. Model. Earth Syst., 11, 3305-3320, 2019.
822 https://doi.org/10.1029/2019MS001790

823 Mayen, J., Polsenaere, P., Lamaud, É., Arnaud, M., Kostyrka, P., Bonnefond, J.-M., Geairon,
824 P., Gernigon, J., Chassagne, R., and Lacoue-Labarthe, T.: Atmospheric CO_2 exchanges
825 measured by eddy covariance over a temperate salt marsh and influence of environmental
826 controlling factors, Biogeosciences, 21, 993–1016, 2024.

827 McLeod, E., Chmura, G. L., Bouillon, S., Salm, R., Björk, M., Duarte, C. M., Lovelock, C.
828 E., Schlesinger, W. H., and Silliman, B. R.: A blueprint for blue carbon: toward an improved
829 understanding of the role of vegetated coastal habitats in sequestering CO_2, Front. Ecol.
830 Environ., 9, 552–560, https://doi.org/10.1890/110004, 2011.

831 Mcowen, C. J., Weatherdon, L. V., Bochove, J.-W. V., Sullivan, E., Blyth, S., Zockler, C.,
832 Stanwell-Smith, D., Kingston, N., Martin, C. S., Spalding, M., and Fletcher, S.: A global map
833 of saltmarshes, Biodivers. Data J., 5, e11764, https://doi.org/10.3897/BDJ.5.e11764, 2017.

834 McVicar, T., Vleeshouwer, J., Van Niel, T., Guerschman, J., and Peña-Arancibia, J. L.:
835 Actual Evapotranspiration for Australia using CMRSET algorithm. Version 1.0, 2022.

836 Mitsch, W. J. and Gosselink, J. G.: The value of wetlands: importance of scale and landscape
837 setting, Ecol. Econ., 35, 25–33, https://doi.org/10.1016/S0921-8009(00)00165-8, 2000.

838 Moffett, K. B., Wolf, A., Berry, J. A., and Gorelick, S. M.: Salt marsh–atmosphere exchange
839 of energy, water vapor, and carbon dioxide: Effects of tidal flooding and biophysical controls,
840 Water Resour. Res., 46, 2010.

841 Nahrawi, H., Leclerc, M. Y., Pennings, S., Zhang, G., Singh, N., and Pahari, R.: Impact of
842 tidal inundation on the net ecosystem exchange in daytime conditions in a salt marsh, Agric.
843 For. Meteorol., 294, 108133, https://doi.org/10.1016/j.agrformet.2020.108133, 2020.

844 Navarro, A., Young, M., Macreadie, P. I., Nicholson, E., and Ierodiaconou, D.: Mangrove
845 and saltmarsh distribution mapping and land cover change assessment for south-eastern
846 Australia from 1991 to 2015, Remote Sens., 13, https://doi.org/10.3390/rs13081450, 2021.

847 Osborne, C. P. and Freckleton, R. P.: Ecological selection pressures for C4 photosynthesis in
848 the grasses. Proc. Roc. Soc. B, 276, https://doi.org/10.1098/rspb.2008.1762, 2009.

849 Otani, S. and Endo, T.: CO_2 flux in tidal flats and salt marshes, Blue Carbon Shallow Coast.
850 Ecosyst. Carbon Dyn. Policy Implement., 223–250, 2019.

851 Owers, C. J., Rogers, K. and Woodroffe, C. D.: Spatial variation of above-ground carbon
852 storage in temperate coastal wetlands. Estuar. Coast. Shelf Sci., 210, 55-67,
853 https://doi.org/10.1016/j.ecss.2018.06.002, 2018
854
855 R Core Team: R: A Language Environment for Statistical Computing. Vienna, Australia,
856 2024.

Reents, S., Möller, I., Evans, B. R., Schoutens, K., Jensen, K., Paul, M., Bouma, T. J., Temmerman, S., Lustig, J., Kudella, M., and Nolte, S.: Species-specific and seasonal differences in the resistance of salt-marsh vegetation to wave impact, Front. Mar. Sci., 9, 2022.

Rosentreter, J. A., Laruelle, G. G., Bange, H. W., Bianchi, T. S., Busecke, J. J. M., Cai, W. J., Eyre, B. D., Forbich, I., Kwon, E. Y., Maavara, T., Moosdorf, N., Najjar, R. G, Sarma, V. V. S. S., Van Dam, B. and Regnier, P.: Coastal vegetation and estuaries are collectively a greenhouse gas sink. Nat. Clim. Chang. 13, 579–587. https://doi.org/10.1038/s41558-023-01682-9, 2023.

Schäfer, K. V. R., Duman, T., Tomasicchio, K., Tripathee, R., and Sturtevant, C.: Carbon dioxide fluxes of temperate urban wetlands with different restoration history, Agric. For. Meteorol., 275, 223–232, https://doi.org/10.1016/j.agrformet.2019.05.026, 2019.

Seyfferth, A. L., Bothfeld, F., Vargas, R., Stuckey, J. W., Wang, J., Kearns, K., Michael, H. A., Guimond, J., Yu, X., and Sparks, D. L.: Spatial and temporal heterogeneity of geochemical controls on carbon cycling in a tidal salt marsh, Geochim. Cosmochim. Acta, 282, 1–18, 2020.

Shepard, C. C., Crain, C. M., and Beck, M. W.: The protective role of coastal marshes: a systematic review and meta-analysis, PLoS ONE, 6, e27374, https://doi.org/10.1371/journal.pone.0027374, 2011.

Smith, J. A. M., Regan, K., Cooper, N. W., Johnson, L., Olson, E., Green, A., Tash, J., Evers, D. C., and Marra, P. P.: A green wave of saltmarsh productivity predicts the timing of the annual cycle in a long-distance migratory shorebird, Sci. Rep., 10, 20658, https://doi.org/10.1038/s41598-020-77784-7, 2020.

Vázquez-Lule, A. and Vargas, R.: Biophysical drivers of net ecosystem and methane exchange across phenological phases in a tidal salt marsh, Agric. For. Meteorol., 300, 108309, https://doi.org/10.1016/j.agrformet.2020.108309, 2021.

Wang, Z. A., Kroeger, K. D., Ganju, N. K., Gonneea, M. E., and Chu, S. N.: Intertidal salt marshes as an important source of inorganic carbon to the coastal ocean, Limnol. Oceanogr., 61, 1916–1931, https://doi.org/10.1002/lno.10347, 2016.

Ward, N. D., Megonigal, J. P., Bond-Lamberty, B., Bailey, V. L., Butman, D., Canuel, E. A., Diefenderfer, H., Ganju, N. K., Goñi, M. A., and Graham, E. B.: Representing the function and sensitivity of coastal interfaces in Earth system models, Nat. Commun., 11, 2458, 2020.

Wei, S., Han, G., Jia, X., Song, W., Chu, X., He, W., Xia, J., and Wu, H.: Tidal effects on ecosystem CO2 exchange at multiple timescales in a salt marsh in the Yellow River Delta, Estuar. Coast. Shelf Sci., 238, 106727, 2020.

Whitfield, A. K.: The role of seagrass meadows, mangrove forests, salt marshes and reed beds as nursery areas and food sources for fishes in estuaries, Rev. Fish Biol. Fish., 27, 75–110, https://doi.org/10.1007/s11160-016-9454-x, 2017.

Xiao, J., Sun, G., Chen, J., Chen, H., Chen, S., Dong, G., Gao, S., Guo, H., Guo, J., Han, S., Kato, T., Li, Y., Lin, G., Lu, W., Ma, M., McNulty, S., Shao, C., Wang, X., Xie, X., Zhang,

Formatted: Font: (Default) Times New Roman
Formatted: Font: (Default) Times New Roman
Formatted: Font: (Default) Times New Roman
Formatted: Font: (Default) Times New Roman
Formatted: Font: (Default) Times New Roman, Not Italic
Formatted: Font: (Default) Times New Roman
Formatted: Font: (Default) Times New Roman, Not Italic
Formatted: Font: (Default) Times New Roman
Formatted: Font: (Default) Times New Roman, Not Bold
Formatted: Font: (Default) Times New Roman
Formatted: Font: (Default) Times New Roman
Formatted: Hyperlink, Font: (Default) Times New Roman, Font colour: Auto, Pattern: Clear
Field Code Changed
Deleted: ¶

X., Zhang, Z., Zhao, B., Zhou, G., and Zhou, J.: Carbon fluxes, evapotranspiration, and water use efficiency of terrestrial ecosystems in China, Agric. For. Meteorol., 182–183, 76–90, https://doi.org/10.1016/j.agrformet.2013.08.007, 2013.